

Modeling of AC Contactors to Improve Life

Liping Guo, Aleck W. Leedy, Sidney Schaaf, Brian Backs, Mark Gabatino, Nathan James, Mike Pintozzi

Abstract— The life expectancy of an AC contactor is adversely affected by electrical arcs and heat rise within the contactor. Electrical arcing results in erosion in the contact material and also results in failures due to welding. To find alternative methods of improving contactor life expectancy and reduce the maximum temperature without adding costs to production, a computer model was created for the contactor using MATLAB and Simulink that simulated the dynamics of the contactor at closing. The model solves equations that use geometries and material properties to estimate contact life and heat generation. The results from the simulation can be used to run a Design of Experiments analysis to find which combinations improve life and reduce maximum temperature without adding significant costs.

Index Terms— AC contactors, Design of Experiments (DOE), MATLAB, and Simulink.

I. INTRODUCTION

AC contactors have been used in industry for many years. Contactors are used in applications that require circuit making and breaking. Applications in industry where AC contactors are used include automatic electrical devices, motor starters, and heaters. The life expectancy of an AC contactor is adversely affected by electrical arcs and heat rise within the contactor [1], [2]. Existing technology, such as arc suppression, improves the life of the contactor by protecting against electrical arcing. However, this solution can be costly for manufacturing and distribution in large quantities. This paper aims to find alternative methods to improve contactor life expectancy and reduce the maximum temperature without adding costs to production.

In the literature, the factors of dynamics, arc erosion, and temperature were modeled individually. Dynamic behavior of an AC contactor was modeled and simulated [3]. A computer model was developed to simulate the contact erosion in three-phase vacuum contactors [4]. Temperature estimation of dc contactors was modeled, and the model was verified using experiments. However, the arc erosion, temperature rise, and dynamics of the movable core are all interconnected and play a role in the life of contactors. This paper describes modeling and simulation of an AC contactor that includes dynamics, arc erosion, and temperature. MATLAB/Simulink simulation has been used to model a variety of systems, such as microwave radiometer [5], and power systems [6].

Manuscript Received June 26, 2013

Liping Guo, Department of Engineering Technology, Northern Illinois University, Still Gym 203, DeKalb,

Aleck W. Leedy, Department of Engineering and Physics, Murray State University, 131 Blackburn Science Building, Murray,

Sidney Schaaf, Hartland Controls, 807 Antec Road, Rock Falls, IL 61071,

Brian Backs, Hartland Controls, 807 Antec Road Rock Falls, IL 61071,

Mark Gabatino, Department of Engineering Technology, Northern Illinois University,

Nathan James, Department of Engineering Technology, Northern Illinois University,

Mike Pintozzi, Department of Engineering Technology, Northern Illinois University,

The model presented solves equations that use geometries and material properties to estimate contactor life and heat generation. The results from the simulation were then used to conduct a Design of Experiments (DOE) analysis to find an optimum point that improves life and reduces maximum temperature without adding significant costs.

II. THEORETICAL ANALYSIS

The factors of arc erosion, temperature rise over time, power factor, and constriction resistance are included in the modeling and simulation. The simulation is modularized into several blocks: magnetic and dynamics of the moveable core, arc erosion, temperature, constriction resistance, variable change due to temperature, and output block. The magnetic and dynamics of the movable core was modeled and simulated based on a model in the literature [3]. In the arc erosion block, the total number of operations and average erosion per operation due to arc erosion were calculated using measured data. The temperature block includes temperature over distance, and temperature rise over time. The block of variable change due to temperature mainly simulates the linear expansion of materials, change in hardness, and resistivity change with respect to temperature.

A. Arc Erosion

The total number of operations and average erosion per operation due to arc erosion were calculated using measured data. The calculation requires a life test on a contactor in order to properly calibrate the results. The measurements to be taken are the total eroded height of contacts at failure and the total number of operations the contactor sustained before failure. In this model, the total eroded height of the contacts was assumed to be the total height of the layer of silver on the contact pads. The total eroded height can be converted to total eroded mass by using the following equation [4]:

$$M_{in} = \pi r^2 \Delta x_{measured} \delta \quad (1)$$

where

M_{in} =Mass loss over lifespan of contactor (measured),

r =Radius of contact pad,

$\Delta x_{measured}$ =Total eroded height of contacts (measured),

and

δ =Material density.

The charge, Q , per operation, can then be found as [4]:

$$Q = i t \quad (2)$$

where

i =Average current value, and

t = Average arcing time per operation.

The charge per operation, the measured number of operations, and the measured eroded mass can then be used to find the erosion rate constant k as described in the following equation [4]:

$$k = \frac{M_{in}}{n_{in} Q} \quad (3)$$

where

n_m = Total number of operations sustained before failure (measured).

The erosion rate constant can be used in the following equation to calculate the average height loss per operation [4]:

$$\Delta x = \frac{kQ}{\pi \delta r^2} \quad (4)$$

where

Δx = Average height loss per operation.

Equation (4) can be converted to average eroded mass per operation [4] as follows:

$$M = \pi r^2 \delta \Delta x. \quad (5)$$

The total number of operations can then be found by using the following equation [2]:

$$n = \frac{\pi D_c^2 \left(h - \frac{D_A}{4} \right) ASCD}{4M} \quad (6)$$

where

D_c = Diameter of contact pad,

D_A = Diameter of arc,

h = Height of contact pad,

$ASCD$ = Arc spot current density, and

M = Mass change per operation due to arcing (in μg).

B. Temperature Distribution Over Contactor Bridge

The calculation of the temperature distribution over the contactor bridge is based on a model developed by Paisios, et al. [7]. This model calculates the maximum temperature that certain parts of the contactor bridge in a one-pole DC contactor can reach given material properties and dimensions. It examines the thermal power as the current passes through the contacts and contactor carrier bridge. It takes into account the material properties of the contactor bridge and contact pads.

The thermal power is calculated from the left and right of the contact indicated by the arrow as shown in Figure 1. The temperature distribution was modeled first to find the temperature reached in the contacts and contactor bridge due to the flow of current. The model then looks at the steady-state temperature difference distribution.

C. Temperature Over Time

The temperature rise output is used to simulate the heat rise with respect to time on the contact pads as there is current flowing through them [7]. The calculation uses the maximum temperature from the temperature distribution over the contact bridge calculation as well as the ambient temperature as follows:

$$T_{Rise} = \left[- (T_{max} - AT) e^{-x} \right] + T_{max} \quad (7)$$

where

T_{max} = Maximum temperature from the temperature distribution calculation, and

AT = Ambient temperature.

Figure 2 shows the output of the temperature over time.

D. Power Factor

Different loads will result in different values of power factor. The inductance or capacitance in the load causes a phase difference between the voltage and current. Power factor is defined as the ratio between the average power and the apparent power. Power factor is included in the model presented.

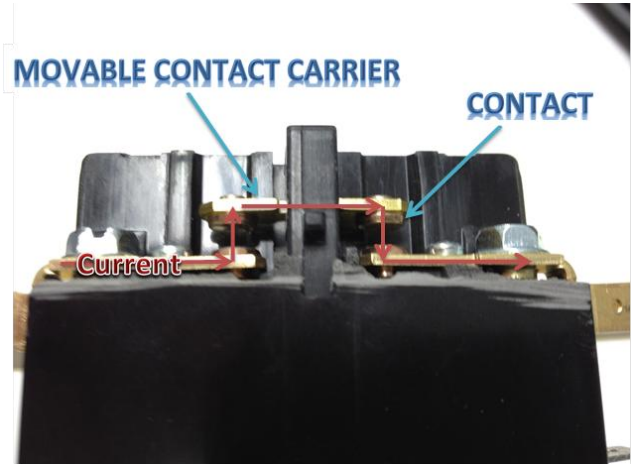


Figure 1. Side view of the contactor.

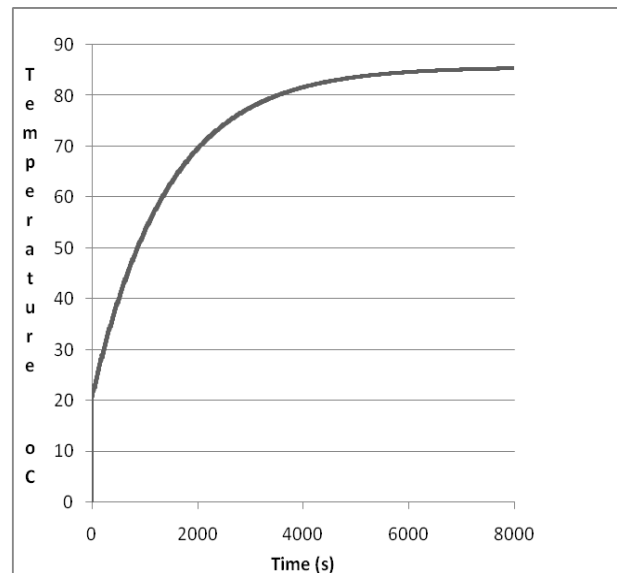


Figure 2. Temperature over time.

E. Constriction Resistance

It was necessary to include constriction resistance in the model to be able to calculate the voltage drop across the contacts [8]. Constriction resistance was found by using the following equation [2]:

$$R_c = \frac{\rho}{2} \sqrt{\frac{\pi H}{F}} \quad (8)$$

where

ρ = Resistivity of contact pad material (Ohm meters),

H = Hardness of contact pad material (Vickers), and

F = Contact holding force (Newtons).

The material hardness for AgCdO (10%) is $6 - 10 \times 10^2$ Nmm⁻² [2]. The hardness is then fed into the model and changed as the temperature increases. The change in hardness due to temperature is found using the following equation [9]:

$$H = Ae^{-BT} \quad (9)$$

where

H =Final hardness (Vickers),
 A =Hardness at $T=0$ Kelvin,
 T =Temperature in Kelvin, and
 B =Softening coefficient.

The contact force for constriction resistance was found by first analyzing the free body diagram (FBD) of the contactor bridge. The FBD when the contactor is closed is shown in Figure 3.

When the contactor is closed, the force necessary for holding the contacts against each other needs to be found. To determine this force, the basic free body diagram in Figure 3 was drawn to show the effective forces acting on the contacts. When the contactor is closed, the cores of the magnetics are resting against each other. Therefore, the weight of the magnetic core can be ignored. The main forces acting on the contacts were the moments about the points of contact, the spring force from the contact spring, and the mass of the contactor carrier bridge. When analyzing the FBD, the following is assumed since it is static [10]:

$$\sum F_x = 0, \sum F_y = 0, \text{ and } \sum M = 0. \quad (10)$$

After analyzing the forces of the FBD shown in Figure 3, the following is found:

$$\sum F_y = 0 = \text{Force}(A) + \text{Force}(C) - \text{Force}(\text{Spring}) - \text{Weight of the Bridge}, \quad (11)$$

and

$$\sum M_A = -\text{Force}(\text{Spring}) * L_{AB} - \text{Weight}_{\text{Bridge}} * L_{AB} + F_C(L_{AB} + L_{BC}) = 0. \quad (12)$$

By looking at the moment about point A, the force acting on point C can be found. This force is the contact holding force. The constriction resistance is then used to find the voltage drop as follows [2]:

$$V_S = IR_C. \quad (13)$$

The result is used in the maximum temperature described in Section II C.

F. Resistivity, Resistance, and Contact Geometries

The resistivity, ρ , used in calculating the constriction resistance also changes with temperature. The linear relationship between resistivity and temperature is found as [2]:

$$\rho_T = \rho_0[1 + \alpha(T - T_0)] \quad (14)$$

where

ρ_T = Resistivity at the given temperature ($\Omega.m$),
 ρ_0 = Initial resistivity ($\Omega.m$),
 α = Temperature coefficient of resistance, to within about 20% up to the metal's melting point,
 T = Temperature ($^\circ\text{C}$), and
 T_0 = Initial temperature ($^\circ\text{C}$).

This linear relationship was used to find the resistance at the given temperature, R_T (Ω), by using the initial resistance, R_0 (Ω). Similarly, the length, width, and height of the contacts and contactor bridge change with temperature in a linear relationship [10]:

$$l_f = \alpha(\Delta T) + l_0 \quad (15)$$

where

l_f = Final length at the given temperature,
 l_0 = Initial length,
 α = Coefficient of expansion, and
 ΔT = Change in temperature.

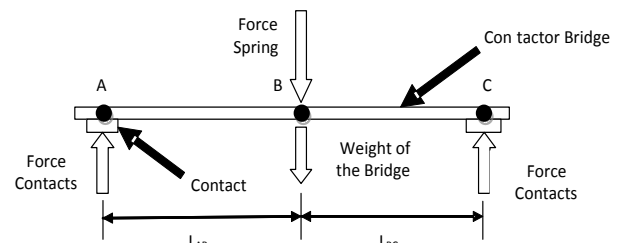


Figure 3. Free body diagram.

III. SIMULATION RESULTS

After running the simulation, the results of the temperature distribution were obtained. The material selected for simulation studies was Silver Cadmium Oxide (AgCdO), which has been the standard contact material in contactors. Figure 4 shows the comparison of maximum temperature for nominal design values using the material of AgCdO, where point A and point C in Figure 3 are seen at approximately 90 mm and 110 mm respectively. Figure 5 shows the comparison of maximum temperature for design values at 10% below nominal design. Figure 6 shows the comparison of maximum temperature for design values at 10% above nominal design.

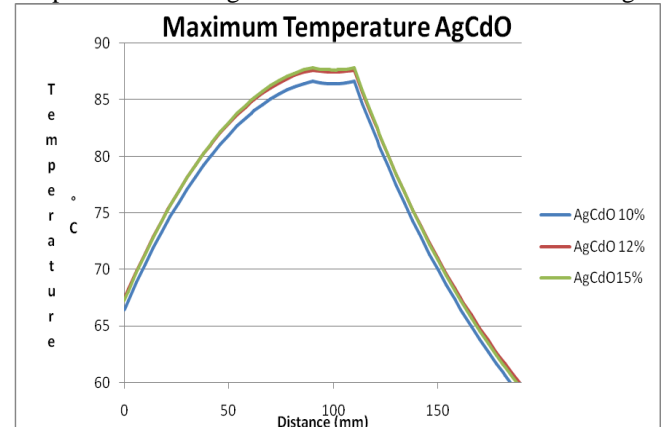


Figure 4. Simulation results of comparison of maximum temperature for nominal design values using AgCdO.

Modeling of AC Contactors to Improve Life

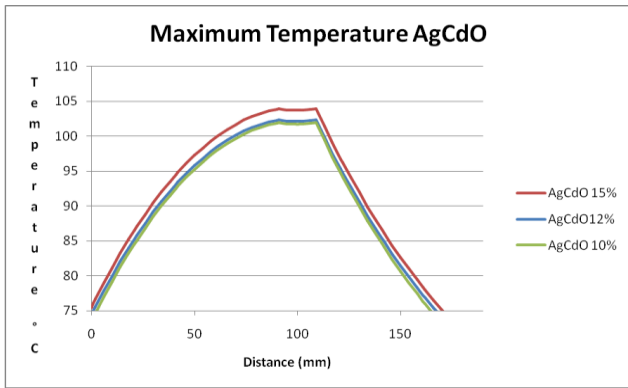


Figure 5. Simulation results of comparison of maximum temperature for design values at 10% below nominal design using AgCdO.

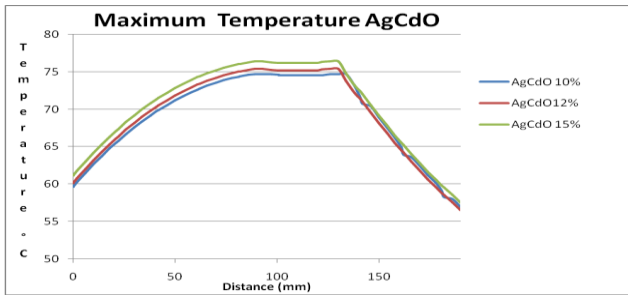


Figure 6. Simulation results of comparison of maximum temperature for design values at 10% above nominal design using AgCdO.

IV. DESIGN OF EXPERIMENT (DOE) ANALYSIS

A Design of Experiments (DoE) analysis was conducted using Design-Expert 8 software. This analysis plots multiple variables and their effect on certain specified responses. These interaction graphs can be used to determine how the variables interact and affect each response. The following parameters were changed at +/- 10% of design value for the DoE analysis:

- Height of contacts (meters),
- Width of contacts (meters),
- Distance between contacts (millimeters),
- Height of contactor bridge (meters),
- Width of contactor bridge (meters),
- Length of contactor bridge (millimeters), and
- Elastic constant of contact springs (Newtons / meter).

These parameters were tested for AgCdO (10%), AgCdO (12%), and AgCdO (15%). The outputs being measured were the number of operations, maximum temperature, and constriction resistance. Figure 7 is a summary of data in Design-Expert 8 that was used for analysis of the AgCdO (10%) test.

The DoE analysis produces 2-axes interaction graphs. The y-axis represents the output response, and the x-axis represents the first input variable. The red line represents the second input variable at +10%, and the black line represents the second input variable at -10%. An optimum point for the two variables can be found if the two lines have an intersection.

The two parameters that had the greatest effect on life and temperature are the height and width of the contacts. Figure 8,

9, and 10 shows the effect of contactor width and height on number of operations, on final temperature, and on constriction resistance, respectively. Table 1 summarizes the results of the DoE analysis with regard to maximum temperature and estimated contactor life for the given materials, each with the height and width of the contacts at +10%.

Design Summary

File Version: 8.0.7.1
 Study Type: Factorial
 Design Type: 2 Level Factorial
 Center Point: 0
 Design Mode: 7FI
 Runs: 128
 Blocks: No Blocks
 Build Time (ms): 5.42

Factor	Name	Units	Type	Subtype	Minimum	Maximum	Coded Values	Mean	Std. Dev.
A	Elastic Constant of the Contact Springs	N/m	Numeric	Continuous	62.307	76.153	-1.000-0.207 1.000+0.76153	69.23	6.923
B	Length of the Contactor Bridge	mm	Numeric	Continuous	24.3	29.7	-1.000-24.3 1.000+29.7	27	2.7
C	Width of the Contactor Bridge	mm	Numeric	Continuous	0.00387	0.00473	-1.000-0.00387 1.000+0.00473	0.0043	0.00043
D	Height of the Contactor Bridge	mm	Numeric	Continuous	0.00132	0.001628	-1.000-0.00132 1.000+0.001628	0.00148	0.000148
E	Distance Between Contacts	mm	Numeric	Continuous	18	22	-1.000-18 1.000+22	20	2
F	Width of the Contacts	mm	Numeric	Continuous	0.0054	0.0066	-1.000-0.0054 1.000+0.0066	0.006	0.0006
G	Height of the Contacts	mm	Numeric	Continuous	0.01269	0.01551	-1.000-0.01269 1.000+0.01551	0.0141	0.00141

Response	Name	Units	Obs	Analysis	Minimum	Maximum	Mean	Std. Dev.	Ratio	Trans	Model
Y1	Number of Operations		128	Factorial	198970	387491	289444	71808.6	1.98775	None	7FI
Y2	Final Temperature	deg C	128	Factorial	74.5525	100.793	86.5249	7.58321	1.35197	None	7FI
Y3	Constriction Resistance	ohms	128	Factorial	0.00063199	0.00061754	0.00064837	8.95952E-006	1.9471	None	7FI

Figure 7. Design summary for DOE analysis.

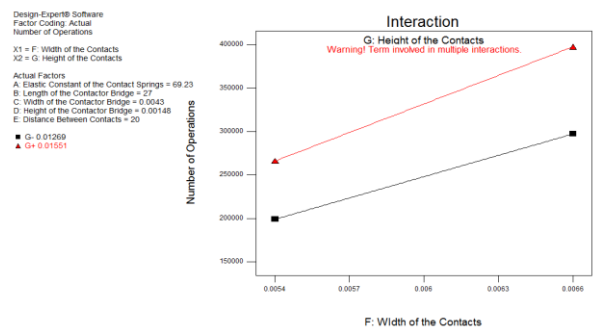


Figure 8. Effect of contact width and height on number of operations.

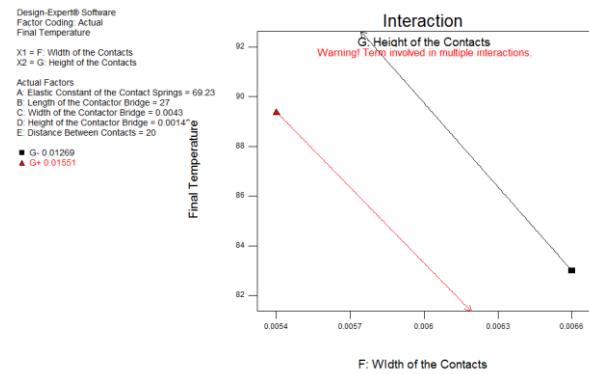


Figure 9. Effect of contact width and height on final temperature.

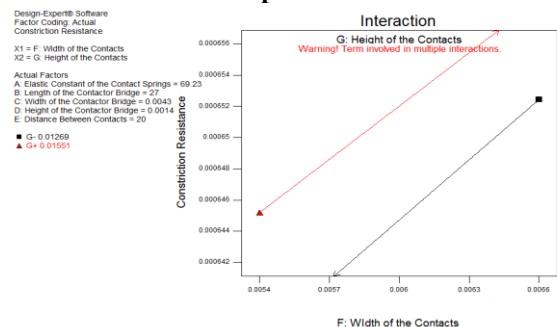


Figure 10. Effect of width and height on constriction resistance.

V. CONCLUSION

The simulation model of AC contactors was presented in this paper. The model can be used to find the maximum temperature that an AC contactor dissipates at a certain current level. The dimensions and materials used in manufacturing the contactor bridge can be changed to see how the maximum temperature changes. Temperature change over the life of an AC contactor can also be observed using the model.

Through the Design of Experiment testing, it was seen that the largest effect on temperature was from the size of the contact pads. The contactor bridge also played a limited role in contact temperature conduction. However, other factors such as overall cost, bounce time, and life should be considered before increasing the size of the contactor.

The modeling and simulation of an AC contactor presented in this paper included the effects of dynamics, arc erosion, and temperature. In the literature, the factors of dynamics, arc erosion, and temperature were only modeled individually. However, the arc erosion, temperature rise, and dynamics of the movable core are all interconnected and play a role in the life of contactors. Therefore, the model presented is an improvement to the existing AC contactor models available in the literature.

Table 1. Summary of DOE results

	AgCdO (10%)	AgCdO (12%)	AgCdO (15%)
Temperature (°C) at + 10% contactor size	74.6	75.2	76.1
Temperature (°C) at - 10% contactor size	100.8	102	103.6
Number of operations at + 10% contactor size	397,491	397,491	414,173
Number of operations at - 10% contactor size	198,969	199,154	207,320

ACKNOWLEDGMENT

This work was supported by Hartland Controls.

REFERENCES

1. M. Braunovic, V. Konchits and N. Myshkin, *Electrical Contacts Fundamentals, Applications, and Technology*, Boca Raton, FL: CRC Press, Taylor & Francis Group, 2007.
2. P. G. Slade, *Electrical Contacts Principles and Applications*, Boca Raton, FL: CRC Press, Taylor & Francis Group, 1999.
3. J. R. Riba Ruiz and A. G. Espinosa, "A computer model for teaching the dynamic behavior of AC contactors," *IEEE Transactions on Education*, vol. 53, no. 2, pp. 248-256, May 2010.
4. J. J. Shea, "Modeling contact erosion in three phase vacuum contactors," *IEEE Transactions on Components, Packaging, and Manufacturing Technology*, vol. 21, no. 4, pp. 556-564, 1998.
5. D. M. Burrage, M. A. Goodberlet and H. L. and Malcom, "Simulating Passive Microwave Radiometer Designs Using Simulink," *Simulation: Transactions of The Society for Modeling and Simulation International*, vol. 78, no. 1, pp. 36-55, 2002.
6. W. Leedy and R. M. Nelms, "A general method used to conduct a harmonic analysis on carrier-based pulse width modulation inverters," *Simulation: Transaction of the Society for Modeling and Simulation International*, vol. 87, no. 3, pp. 205-220, 2011.
7. M. P. Paisios, C. G. Karagiannopoulos and P. D. Bourkas, "Model for temperature estimation of dc-contactors with double-break main contacts," *Simulation Modelling Practice and Theory*, vol. 15, no. 5, pp. 503-512, 2007.

8. J. D. Lavers, "Constriction resistance at high signal frequencies," *IEEE Transactions on Components and Packaging Technology*, vol. 25, no. 3, pp. 446-452, 2002.
9. H. D. Merchant, G. S. Murty, S. N. Bahadur, L. T. Dwivedi and Y. Mehrotra, "Hardness-temperature relationships in metals," *Journal of materials science*, pp. 437-442, 1973.
10. G. Thiagarajan and K. Deshmukh, *Mechanics of materials*, 4th Ed., Mission, KS: SDC Publications, 2010.

AUTHORS PROFILE



Liping Guo received the B.E. degree in Automatic Control from Beijing Institute of Technology, Beijing, China in 1997, the M.S. and Ph.D. degrees in Electrical and Computer Engineering from Auburn University, AL, USA in 2001 and 2006 respectively.

She is currently an Assistant Professor in the Electrical Engineering Technology Program in the Department of Technology at the Northern Illinois University. Her research interests are mainly in the area of power electronics, power systems, renewable energy, embedded systems and control. Dr. Guo is a member of the IEEE Industrial Electronics Society and a member of the honor society of Phi Kappa Phi.



Aleck W. Leedy received the B.S. degree in electrical engineering and the M.S. degree in mining engineering from the University of Kentucky, Lexington, KY, and the Ph.D. degree in electrical engineering from Auburn University, Auburn, AL, in 1996, 2001, and 2006, respectively. He also received the Master of Applied Mathematics degree from Auburn University, Auburn, AL, in 2006.

He is currently an Assistant Professor of electrical engineering in the Department of Engineering and Physics at Murray State University, Murray, KY. His teaching and research interests are in the areas of power systems, power electronics, and electric machines.

Dr. Leedy is a registered professional engineer in the Commonwealth of Kentucky. He is a member of IEEE, Order of the Engineer, IEEE Industry Applications Society, and IEEE Industrial Electronics Society.